

TMUP-HEL-9805

hep-ph/9804400

Three flavor neutrino oscillation analysis of the Superkamiokande atmospheric neutrino data

Osamu Yasuda*

Department of Physics, Tokyo Metropolitan University

Minami-Osawa, Hachioji, Tokyo 192-0397, Japan

(April, 1998)

Abstract

Superkamiokande atmospheric neutrino data for 414 days are analyzed in the framework of three flavor oscillations with mass hierarchy. It is shown that the best fit point is very close to the pure maximal $\nu_\mu \leftrightarrow \nu_\tau$ case and $\Delta m^2 \simeq 7 \times 10^{-3}$ eV². The allowed region at 90 %CL is given and the implications to the long baseline experiments are briefly discussed.

14.60.P, 26.65, 28.41, 96.60.J

Typeset using REVTEX

*Email: yasuda@phys.metro-u.ac.jp

Recent data from atmospheric neutrino experiments [1] and especially the Superkamiokande experiment [1,2] provide very strong evidence for neutrino oscillations. In [3] the atmospheric neutrino data for 414 days have been analyzed in the framework of two flavor oscillations $\nu_\mu \leftrightarrow \nu_\tau$ or $\nu_\mu \leftrightarrow \nu_s$, and it has been shown that both scenarios give a good fit to data. In this paper we extend the analysis of [3] to the case of three flavor oscillations. (For quantitative three flavor analysis of atmospheric neutrinos, see [4–7].) In case of general three flavor mixings the data from the CHOOZ experiment [8] gives a strong constraint to any channel which involves ν_e , so we include the combined χ^2 of the reactor experiments CHOOZ, Bugey [9] and Krasnoyarsk [10] in our χ^2 analysis.

The pattern of mass squared differences with hierarchy can be classified into two cases which are depicted in Fig. 1. As in [6] we ignore the smaller mass squared difference, since it is expected to be of order 10^{-5} eV 2 or 10^{-10} eV 2 to account for the solar neutrino deficit [11] and therefore too small to be relevant to atmospheric neutrinos. Furthermore we put the CP violating phase $\delta = 0$ for simplicity. Then we are left with three parameters $(m^2, \theta_{13}, \theta_{23})$ in the standard parametrization [12]. As has been noted in [6], two schemes (a) and (b) in Fig. 1 are related by exchanging the sign of m^2 , and the case with $m^2 > 0$ stands for the scheme (a) while the one with $m^2 < 0$ for (b) in Fig. 1. To evaluate the number of events, we have integrated numerically the Schrödinger equation

$$i \frac{d}{dx} \begin{pmatrix} \nu_e(x) \\ \nu_\mu(x) \\ \nu_\tau(x) \end{pmatrix} = \left[U \text{diag} \left(0, 0, \frac{m^2}{2E} \right) U^{-1} + \text{diag} (0, 0, A(x)) \right] \begin{pmatrix} \nu_e(x) \\ \nu_\mu(x) \\ \nu_\tau(x) \end{pmatrix}, \quad (1)$$

where

$$U \equiv \begin{pmatrix} U_{e1} & U_{e2} & U_{e3} \\ U_{\mu 1} & U_{\mu 2} & U_{\mu 3} \\ U_{\tau 1} & U_{\tau 2} & U_{\tau 3} \end{pmatrix} = \begin{pmatrix} c_{13} & 0 & s_{13} \\ -s_{23}s_{13} & c_{23} & s_{23}c_{13} \\ -c_{23}s_{13} & -s_{23} & c_{23}c_{13} \end{pmatrix} \quad (2)$$

is an orthogonal matrix, E is the neutrino energy, $A(x) \equiv \sqrt{2}G_F N_e(x)$ stands for the matter effect in the Earth [13]. The way to obtain the numbers of events is exactly the same as in

[3], and we refer to [3] for details. In [3] two quantities have been introduced to perform a χ^2 analysis. One is the double ratio [14]

$$R \equiv \frac{(N_\mu/N_e)|_{\text{osc}}}{(N_\mu/N_e)|_{\text{no-osc}}} \quad (3)$$

where the quantities $N_{e,\mu}$ are the numbers of e -like and μ -like events. The numerator denotes numbers with oscillation probability obtained by (1), while the denominator the numbers expected with oscillations switched off. The other one is the quantity on up-down flux asymmetries for α -like ($\alpha=e,\mu$) events (See also [15–18].) and is defined by

$$Y_\alpha \equiv \frac{(N_\alpha^{-0.2}/N_\alpha^{+0.2})|_{\text{osc}}}{(N_\alpha^{-0.2}/N_\alpha^{+0.2})|_{\text{no-osc}}}, \quad (4)$$

where $N_\alpha^{-\eta}$ denotes the number of α -like events produced in the detector with zenith angle $\cos \Theta < -\eta$, while $N_\alpha^{+\eta}$ denotes the analogous quantity for $\cos \Theta > \eta$, where η is defined to be positive. Superkamiokande divides the $(-1, +1)$ interval in $\cos \Theta$ into five equal bins, so we choose $\eta = 0.2$ in order to use all the data in the other four bins. Thus χ^2 for atmospheric neutrinos is defined by

$$\chi_{\text{atm}}^2 = \sum_E \left[\left(\frac{R^{SK} - R^{\text{th}}}{\delta R^{SK}} \right)^2 + \left(\frac{Y_\mu^{SK} - Y_\mu^{\text{th}}}{\delta Y_\mu^{SK}} \right)^2 + \left(\frac{Y_e^{SK} - Y_e^{\text{th}}}{\delta Y_e^{SK}} \right)^2 \right], \quad (5)$$

where the sum is over the sub-GeV and multi-GeV cases, the measured Superkamiokande values and errors are denoted by the superscript “SK” and the theoretical predictions for the quantities are labeled by “th”. In [3] a χ^2 analysis has been performed using the quantities R and Y ’s, or using Y ’s only. Throughout this paper we use the quantities R and Y ’s to get narrower allowed regions for the parameters. We have to incorporate also the results of the reactor experiments. We define the following χ^2 :

$$\chi_{\text{reactor}}^2 = \sum_{j=1,12}^{\text{CHOOZ}} \left(\frac{x_j - y_j}{\delta x_j} \right)^2 + \sum_{j=1,60}^{\text{Bugey}} \left(\frac{x_j - y_j}{\delta x_j} \right)^2 + \sum_{j=1,8}^{\text{Krasnoyarsk}} \left(\frac{x_j - y_j}{\delta x_j} \right)^2, \quad (6)$$

where x_i are experimental values and y_i are the corresponding theoretical predictions, and the sum is over 12, 60, 8 energy bins of data of CHOOZ [8], Bugey [9] and Krasnoyarsk [10], respectively. There are 6 atmospheric and 80 reactor pieces of data in $\chi^2 \equiv \chi_{\text{atm}}^2 + \chi_{\text{reactor}}^2$ and 3 adjustable parameters, m^2 , θ_{13} and θ_{23} , leaving 83 degrees of freedom.

Using the same parametrization as that in [6], the results for the allowed region of the mixing angles (θ_{13} , θ_{23}) are given for various values of m^2 in Figs. 2 and 3. The results for $m^2 > 0$ and $m^2 < 0$ are almost the same. It is remarkable that, unlike in the case [6] of the Kamiokande data [14], the Superkamiokande data strongly favor $\nu_\mu \leftrightarrow \nu_\tau$ oscillations. This is not only because we have included the combined χ^2_{reactor} of the reactor experiments but also because the Superkamiokande data themselves favor $\nu_\mu \leftrightarrow \nu_\tau$ [19]. This result disagrees with [20] in which it was claimed that pure $\nu_\mu \leftrightarrow \nu_e$ gives a good fit to the Superkamiokande data.

The best fit is obtained for $(m^2, \tan^2 \theta_{13}, \tan^2 \theta_{23}, \chi^2) = (7 \times 10^{-3} \text{ eV}^2, 1.1 \times 10^{-2}, 0.93, 71.8)$ for $m^2 > 0$ and $(-7 \times 10^{-3} \text{ eV}^2, 1.5 \times 10^{-2}, 1.1, 71.4)$ for $m^2 < 0$, respectively. $\chi^2_{\text{min}} = (\chi^2_{\text{atm}})_{\text{min}} + (\chi^2_{\text{reactor}})_{\text{min}} = 4.2 + 67.2 = 71.4$ indicates that a fit to data is good for 83 degrees of freedom at the best fit point. The allowed region for m^2 with θ_{13}, θ_{23} unconstrained is given in Fig. 4, where $\Delta\chi^2 \equiv \chi^2_{\text{atm}} + \chi^2_{\text{reactor}} - (\chi^2_{\text{atm}} + \chi^2_{\text{reactor}})_{\text{min}} < 3.5, 6.3, 11.5$ corresponds to 1σ , 90 % CL and 99 % CL, respectively.. The allowed region for $|m^2|$ at 99% CL is $4 \times 10^{-4} \text{ eV}^2 \lesssim |m^2| \lesssim 1.7 \times 10^{-2} \text{ eV}^2$. It should be noted that the large m^2 limit is excluded even at 99% CL because of high statistics of the Superkamiokande data, unlike in the case of Kamiokande data [6].

Finally, let us discuss briefly the implications of the present analysis to the long baseline experiments [21–23]. One of the interesting questions in these long baseline experiments is whether ν_e can be observed from $\nu_\mu \leftrightarrow \nu_e$ oscillations which could be present as a fraction of the full three flavor oscillations. The probability $P(\nu_\mu \leftrightarrow \nu_e)$ in our scheme is given by

$$P(\nu_\mu \leftrightarrow \nu_e) = 4|U_{e3}|^2|U_{\mu 3}|^2 \sin^2 \left(\frac{\Delta m^2 L}{4E} \right), \quad (7)$$

where L stands for the path length of neutrinos. The factor $4|U_{e3}|^2|U_{\mu 3}|^2$ corresponds to $\sin^2 2\theta$ in the two flavor framework, so by substituting this quantity in a $(\Delta m^2, \sin^2 2\theta)$ plot we can examine the possibility of observing ν_e . The maximum values of the factor $4|U_{e3}|^2|U_{\mu 3}|^2$ in the allowed region at 90 % CL and 99 % CL are given in Table. 1, respectively. In general it is difficult for the long baseline experiments [21–23] to see appearance of ν_e .

In particular, for the K2K experiment, which could probe the region of $|m^2|$ as low as 3×10^{-3} eV² for $\nu_\mu \leftrightarrow \nu_e$ oscillations [24], it seems very difficult to observe appearance of ν_e and disappearance of $\nu_\mu \leftrightarrow \nu_\mu$ has to be searched for at least in the first stage of their experiment. On the other hand, if 5×10^{-4} eV² $\lesssim |m^2| \lesssim 1.0 \times 10^{-3}$ eV², there is a chance for KamLAND [25] to see a positive signal in a disappearance experiment of $\bar{\nu}_e \leftrightarrow \bar{\nu}_e$.

In conclusion, we have analyzed the Superkamiokande atmospheric neutrino data in the framework of the three flavor oscillations with mass hierarchical ansatz. We have given a allowed region at a certain confidence level for the mass squared difference and the mixing angles. The data strongly favor $\nu_\mu \leftrightarrow \nu_\tau$ oscillations and therefore the most promising way in the long baseline experiments is to search for appearance of $\nu_\mu \rightarrow \nu_\tau$ if ν_τ can be produced, or to look for disappearance of $\nu_\mu \leftrightarrow \nu_\mu$ if ν_τ cannot be produced.

The author would like to thank H. Minakata for discussions, R. Foot for many useful communications and Center for Theoretical Physics, Yale University for their hospitality during part of this work. This research was supported in part by a Grant-in-Aid for Scientific Research of the Ministry of Education, Science and Culture, #09045036.

REFERENCES

- [1] Y. Totsuka, Talk at *XVIII International Symposium on Lepton-Photon Interactions*, July, Hamburg, Germany (<http://www.desy.de/lp97-docs/proceedings/lp22/lp22.ps>).
- [2] E. Kearns, Talk at *News about SNUS*, ITP Workshop, Santa Barbara, Dec. 1997, <http://www.itp.ucsb.edu/online/snu/kearns/oh/all.html>); hep-ex/9803007; Superkamiokande Collaboration, hep-ex/9803006.
- [3] R. Foot, R. R. Volkas and O. Yasuda, hep-ph/9801431, Phys. Rev. **D** (in press).
- [4] O. Yasuda, hep-ph/9602342; hep-ph/9706546.
- [5] S.M. Bilenky, C. Giunti and C.W. Kim, Astropart. Phys. **4** (1996) 241; C. Giunti, C.W. Kim and M. Monteno, hep-ph/9709439.
- [6] G.L. Fogli, E. Lisi, D. Montanino and G. Scioscia, Phys. Rev. **D55** (1997) 4385.
- [7] M. Narayan, G. Rajasekaran and S. Uma Sankar, Phys. Rev. **D56** (1997) 437.
- [8] CHOOZ Collaboration, M. Apollonio et al., hep-ex/9711002.
- [9] B. Ackar et al., Nucl. Phys. **B434**, (1995) 503.
- [10] G. S. Vidyakin et al., JETP Lett. **59**, 390 (1994).
- [11] See, e.g., J.N. Bahcall, R. Davis, Jr., P. Parker, A. Smirnov, R. Ulrich eds., *SOLAR NEUTRINOS: the first thirty years* Reading, Mass., Addison-Wesley, 1994 and references therein.
- [12] Review of Particle Physics, Particle Data Group, Phys. Rev. **D54** (1996) 1.
- [13] S. P. Mikheyev and A. Smirnov, Nuovo Cim. **9C** (1986) 17; L. Wolfenstein, Phys. Rev. **D17** (1978) 2369.
- [14] Kamiokande Collaboration, K.S. Hirata et al., Phys. Lett. **B280**, 146 (1992); Kamiokande Collaboration, Y. Fukuda et al., Phys. Lett. **B335**, 237 (1994).

- [15] J. Bunn, R. Foot and R. R. Volkas, Phys. Lett. **B413**, 109 (1997).
- [16] J. W. Flanagan, J. G. Learned and S. Pakvasa, Phys. Rev. **D57**, 2649 (1998).
- [17] R. Foot, R. R. Volkas and O. Yasuda, Phys. Rev. **D57**, 1345 (1998); hep-ph/9710403, Phys. Lett. **B** (in press).
- [18] G. L. Fogli, E. Lisi, A. Marrone, and D. Montanino, hep-ph/9711421.
- [19] Notice that Figs. 2 and 3 do not have allowed region toward the right side even for $|m^2| < 10^{-3}$ eV² where the reactor experiments give no constraint.
- [20] M.C. Gonzalez-Garcia, H. Nunokawa, O.L.G. Peres, T. Stanev and J.W.F. Valle, hep-ph/9801368.
- [21] K2K experiment, <http://pnahp.kek.jp/>.
- [22] MINOS experiment, <http://www.hep.anl.gov/NDK/HyperText/numi.html>.
- [23] ICARUS experiment, <http://www.aquila.infn.it/icarus/>.
- [24] K. Nishikawa, preprint INS-Rep.924 (1992).
- [25] KamLAND experiment, <http://www.awa.tohoku.ac.jp/html/KamLAND/>.

Figures

Fig.1 The hierarchical neutrino mass squared differences. The scenarios (a) and (b) are related by exchanging $m^2 \leftrightarrow -m^2$. They are equivalent in vacuum but physically inequivalent in matter.

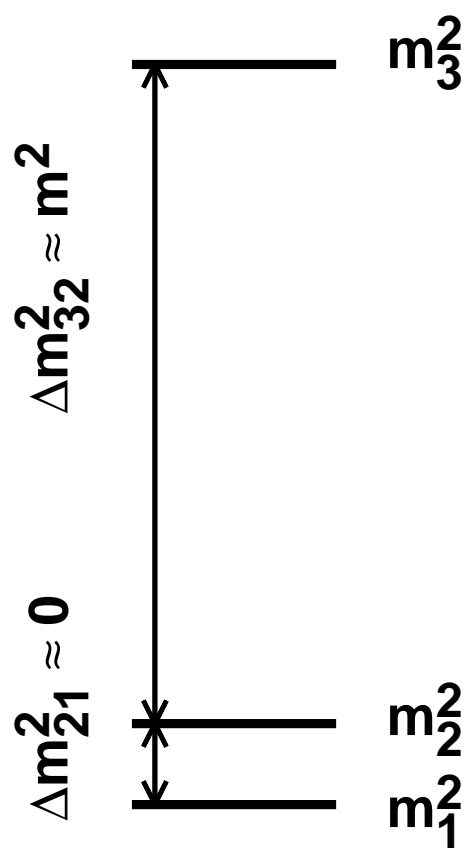
Fig.2 Three flavor analysis of Superkamiokande atmospheric neutrino data and the reactor experiments, CHOOZ, Bugey and Krasnoyarsk. Scenario (a) in Fig. 1 is assumed. The solid, dashed, dotted lines represent 68 % CL, 90 % CL, 99 % CL, respectively for degree of freedom = 3. The right side of each panel corresponds asymptotically to pure $\nu_\mu \leftrightarrow \nu_e$ oscillations and the lower side to pure $\nu_\mu \leftrightarrow \nu_\tau$ oscillations

Fig.3 As in Fig. 2, but the scenario (b) in Fig. 1 is assumed.

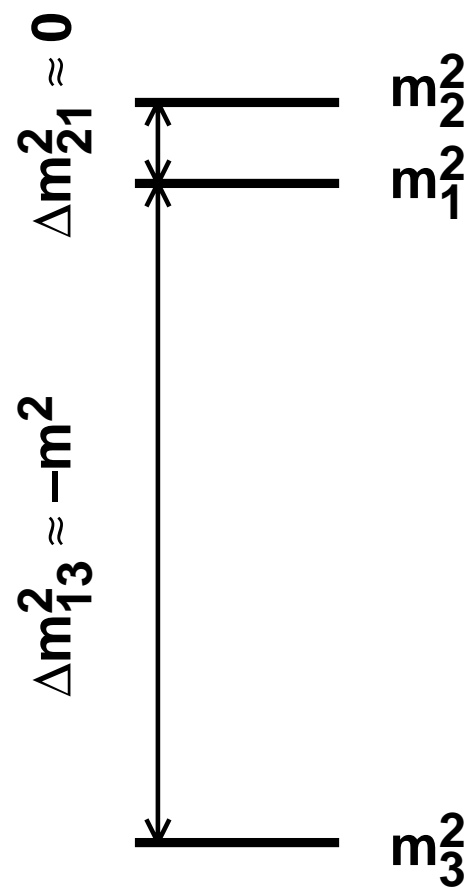
Fig.4 Value of $\Delta\chi^2 \equiv \chi^2_{\text{atm}} + \chi^2_{\text{reactor}} - (\chi^2_{\text{atm}} + \chi^2_{\text{reactor}})_{\text{min}} = \chi^2_{\text{atm}} + \chi^2_{\text{reactor}} - 71.4$. The solid, dash-dotted, dotted lines represent the scenarios (a), (b) and the two flavor case with maximal $\nu_\mu \leftrightarrow \nu_\tau$ mixing, respectively.

m^2	$(4 U_{e3} ^2 U_{\mu 3} ^2)_{\max}$ at 90%CL	$(4 U_{e3} ^2 U_{\mu 3} ^2)_{\max}$ at 99%CL
$3.7 \times 10^{-4}\text{eV}^2$	0.00	0.14
$4.2 \times 10^{-4}\text{eV}^2$	0.00	0.33
$5.6 \times 10^{-4}\text{eV}^2$	0.30	0.53
$7.5 \times 10^{-4}\text{eV}^2$	0.50	0.61
$1.0 \times 10^{-3}\text{eV}^2$	0.50	0.65
$1.8 \times 10^{-3}\text{eV}^2$	0.16	0.29
$3.2 \times 10^{-3}\text{eV}^2$	0.08	0.13
$5.6 \times 10^{-3}\text{eV}^2$	0.07	0.08
$7.5 \times 10^{-3}\text{eV}^2$	0.10	0.12
$1.0 \times 10^{-2}\text{eV}^2$	0.09	0.13
$1.3 \times 10^{-2}\text{eV}^2$	0.00	0.08
$1.8 \times 10^{-2}\text{eV}^2$	0.00	0.07
$-3.7 \times 10^{-4}\text{eV}^2$	0.00	0.11
$-4.2 \times 10^{-4}\text{eV}^2$	0.00	0.38
$-5.6 \times 10^{-4}\text{eV}^2$	0.47	0.59
$-7.5 \times 10^{-4}\text{eV}^2$	0.56	0.70
$-1.0 \times 10^{-3}\text{eV}^2$	0.57	0.71
$-1.8 \times 10^{-3}\text{eV}^2$	0.20	0.32
$-3.2 \times 10^{-3}\text{eV}^2$	0.09	0.14
$-5.6 \times 10^{-3}\text{eV}^2$	0.07	0.09
$-7.5 \times 10^{-3}\text{eV}^2$	0.09	0.12
$-1.0 \times 10^{-2}\text{eV}^2$	0.09	0.13
$-1.3 \times 10^{-2}\text{eV}^2$	0.00	0.08
$-1.8 \times 10^{-2}\text{eV}^2$	0.00	0.07

Table. 1 Maximum values of the coefficient in the probability $P(\nu_\mu \rightarrow \nu_e) = 4|U_{e3}|^2|U_{\mu 3}|^2 \sin^2(\Delta m^2 L/4E)$ allowed at a certain confidence level of $\chi^2_{\text{atm}} + \chi^2_{\text{reactor}}$.



scenario (a)



scenario (b)

Fig.1

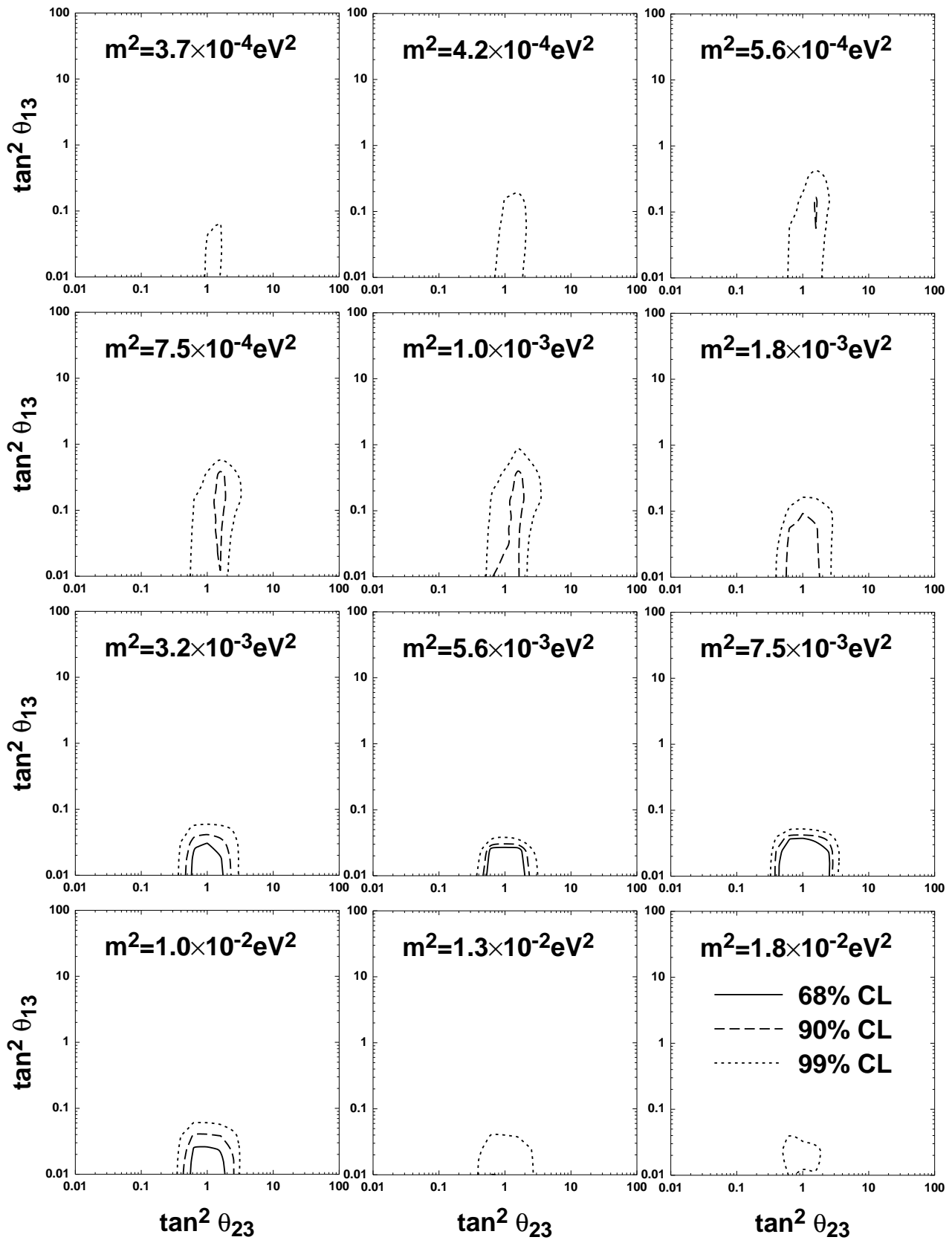


Fig.2

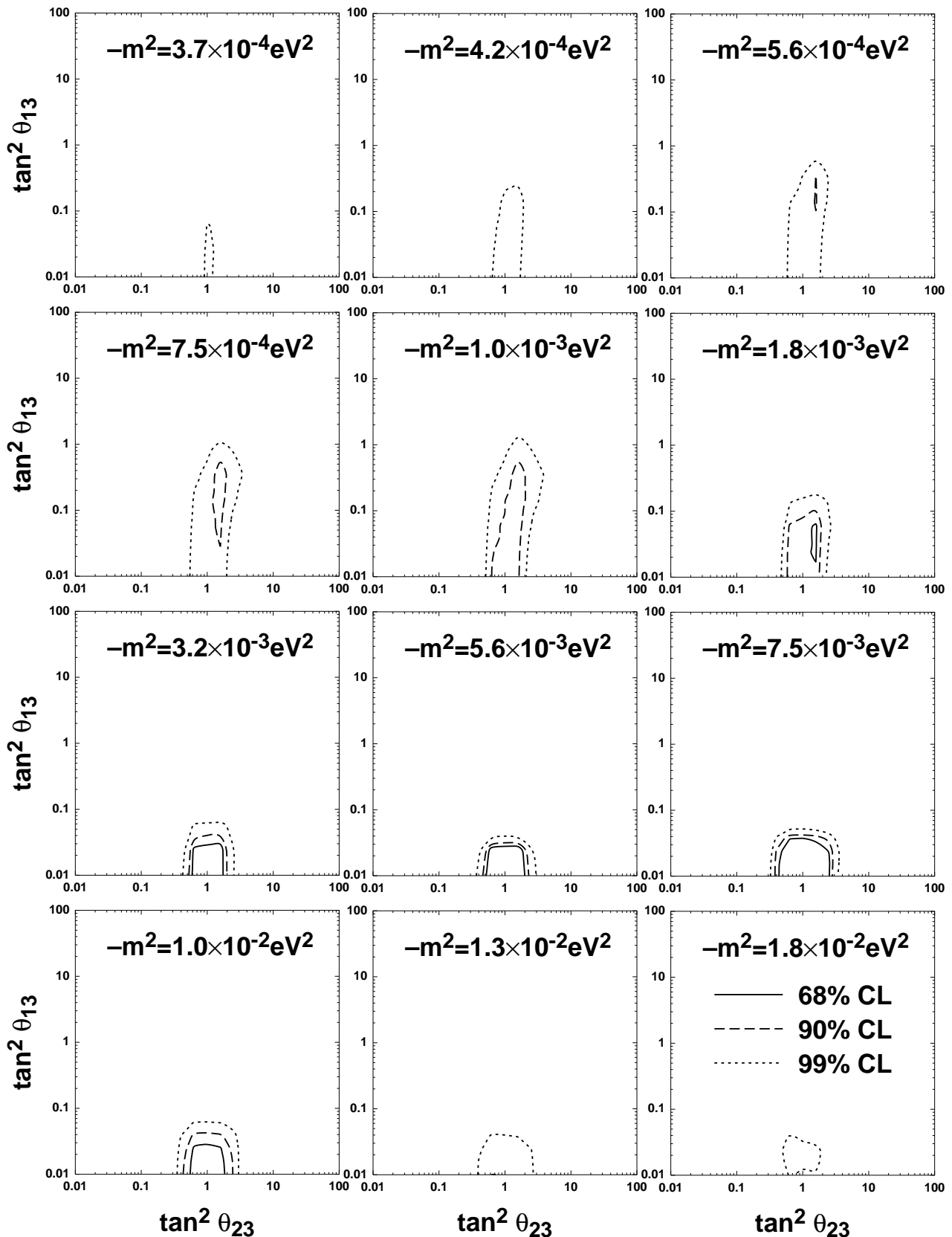


Fig.3

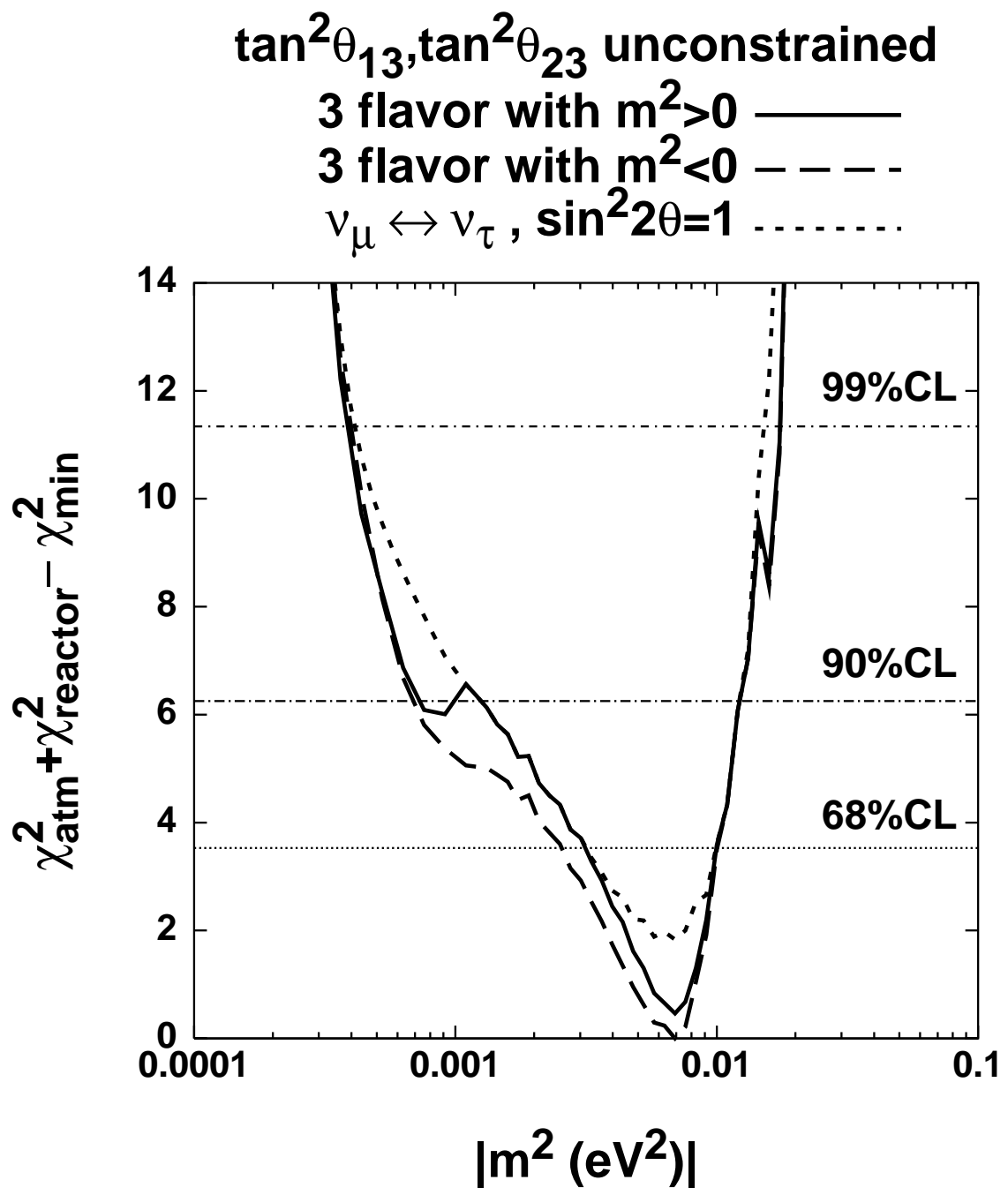


Fig.4